ISSN: 0976-9102 (ONLINE)
DOI: 10.21917/ijivp.2023.0445

COV-CT-NET - A DEEP LEARNING MODEL FOR COVID-19, COMMUNITY-ACQUIRED PNEUMONIA DETECTION USING CT IMAGES

Abul Hasnat[1], Mangalmay Das[2], Santanu Halder[3] and Debotosh Bhattacharjee[4]

[1]*Department of Computer Science and Engineering, Government College of Engineering and Textile Technology, Berhampore, India*
[2]*Department of Computer Science and Engineering, Murshidabad College of Engineering and Technology, India*
[3]*Department of Computer Science and Engineering, Government College of Engineering and Leather Technology, Kolkata, India*
[4]*Department of Computer Science and Engineering, Jadavpur University, India*

Abstract

The world has witnessed the deadly impact of the Novel Corona Virus (COVID-19), claiming millions of lives since its outbreak in early December 2019. Early virus detection plays a crucial role in controlling this highly contagious disease. Though Reverse Transcription Polymerase Chain Reaction (RT-PCR) is the current standard for confirmation of COVID-19, it is time-consuming. Computed Tomography (CT) imaging of the lungs can preferably be used for fast diagnosis of the disease as it is more sensitive and can detect complications. Due to the unavailability of adequate expertise, a deep learning-based model on CT images is a potential solution for fast detecting SARS Cov2 virus. In this study, we developed a simple but robust Convolution Neural Network model with multiclass detection ability between normal lungs, COVID-19 infected lungs and any other Community-Acquired Pneumonia (CAP) infection using Chest CT images. It is tested on a publicly available dataset, COVID-CT-MD and it achieved slice level accuracy of 99% on test dataset. We also attempted slice-level prediction of the unlabelled slices available in the dataset of COVID-19 and CAP cases.

Keywords:

COVID-19 Detection, CAP, CT Imaging, CNN, Deep Learning

1. INTRODUCTION

The world has been going through a painful pandemic since late 2019 with the manifold impact of the novel Corona virus (COVID-19) on socio, economic and human lives. According to World Health Organization (WHO), as of January 2023, there are about 75.2 million confirmed cases of COVID-19, of which 6 million deaths caused by the virus alone. In India, 4.4 million confirmed cases and half million deaths are recorded [1] officially. This record is sufficient to recognize the overwhelming effect of this contagious virus. Moreover, several variants of this virus come in different times and regions. Reverse Transcription Polymerase Chain Reaction (RT-PCR) is currently the gold standard for COVID-19 confirmation [2]. This method requires physical sample for testing. It comes at the expense of time. The test centres providing the RT-PCR testing facility are also limited, Also, RT-PCR testing lacks in identifying severity/stage of the disease [3].

The application of image processing on medical imaging has played important role in diagnosing different symptoms. Chest Radiography (CR) and Computed Tomography (CT) may be used for the early detection of COVID-19 as the images are highly correlated with disease severity [4] [5]. Although CR can assess the extent of COVID-19 involvement, higher sensitivity of CT imaging provides more accuracy in detecting complications [6]. Inadequate expertise and unavailability of knowledgeable workforce in a pandemic situation, a machine-learning model may be a preferable solution. An imaging-based AI model is not only limited to provide the diagnosis of COVID-19 but also a potential solution for any future pandemics when there may not be any rapid tests like RT-PCR.

The most visible primary image patterns in COVID-19 affected lungs are Ground Glass Opacities (GGO) and consolidation [7] [8] [9] [10] [11]. The peripheral location of opacities with rounded morphology is very common in COVID-19 affected lung images [5] [7]. Deep Learning (DL) is an effective method in computer vision tasks- i.e. detecting these imaging patterns [3] [12] [13] [14]. In recent years, application of DL has shown very good results in radiology images for classification, segmentation, detection, and other tasks [3] [15]. DL utilizes target lesions and can be applied to CT scan images, enhancing feature detection and improving diagnosis efficiency [3] [15]. Medical images come with a variety of noises like background clutter, motion artifact, noises due to device calibration, etc. [16]. In such cases, DL is a suitable tool for identification, extraction, classification, etc, of features of interest [3] [13].

In the literature, a few machine-learning models are reported for detecting the COVID-19 based on CT volume imaging. In 2020, Yang, Shuyi, et al. [17] reported that DenseNet works on high-resolution CT images to classify COVID-19 affected cases and normal cases. They used a dataset having 300 to 500 axial image slices per person. The dataset contained 149 normal cases and 146 COVID-19 infected cases. CT scans with visible Ground Glass Opacities (GGO) and GGO with consolidation are used for the COVID-19 class in the training set. For healthy cases, lungs with pulmonary parenchyma are used. Taking the threshold value 0.8, the study reported 95% and 92% accuracy on the validation set and test set respectively. The study did not consider other pathogen pneumonia like CAP cases.

In 2020, Wang et al. [18] reported a CNN model, introduced as Covid-Net, to classify between Normal case, COVID-19 case and Non-COVID Pneumonia case based on CR images. They used publicly available dataset known as COVIDx. It is collection of images from five different data repositories with 13975 images across 13870 subjects. The model uses a projection-expansion-projection design pattern. The model is pre-trained using the ImageNet dataset and then trained on the COVIDx dataset. They used batch size of 64 and patience of 10 for early stopping. They reported 91% sensitivity in detecting COVID-19 cases. The COVIDx dataset has a very few COVID-19 CR images.

In 2020, Shaoping Hu et al. [19] proposed a weakly supervised model with five convolution layers inspired by VGG model for multiclass COVID-19 infection detection. They used CT images using TCIA (Cancer Imaging Archive) dataset. Fixed-size sliding

window is used for image enhancement that overcomes data bias from scanners of different centres. For lung segmentation, UNET is used. To detect lesions of varying size and different location, the intermediate feature maps are used from 3rd, 4th and 5th convolution layers. These intermediate feature maps are fed into weakly supervised convolution layer. It uses 1x1 convolution and Global Max Pooling. The prediction score generated from each weakly supervised layer is aggregated to make the final decision. The study reported accuracy of 84.3% in classifying COVID-19, CAP, and Non-Pneumonia (NP) cases. But the model is not discriminative enough for separating CAP and COVID-19.

In the same year 2020, Mahmud et al. [20] proposed CovXNet to detect COVID-19 using CR image. CovXNet comprises four networks trained and optimized using four different input size of 256x256, 128x128, 64x64 and 32x32. It captures the consolidated and diffusely distributed infected regions. The dilated convolution operation with varying dilation rates is applied in each network. Then these four optimized networks are stacked to form a meta-learner to predict final output. They tested the model on a combined dataset comprising images from a) Mendeley dataset from China- it is publicly available and consists of normal, non-covid viral pneumonia, non-covid bacterial pneumonia class, b) another dataset from Bangladesh with COVID-19 cases only. They used the combined dataset for experimentation with 305 CR images from each class. Initially the model trained with CR images of normal cases, then viral/bacterial pneumonia cases and lastly with COVID-19 infected images. It has some additional fine-tuning layers. They reported 90.2% accuracy but the model used very few COVID-19 infected CR images.

In 2021, a new Feature Pyramid Network (FPN) is proposed by Rahimzadeh et al. [21] that uses ResNet50V2 as backbone model. FPN is primarily build to detect small objects, the authors use this as a feature extractor in five depth levels of ResNet50V2. To preserve location information in top-down pathway of FPN, lateral connections between reconstructed layers and the corresponding feature maps are used. The five level features fed into dense layer with two output neurons in each level. The outputs layer consists of ten neurons. Finally, Soft-Max activation is used for classification. They used the COVID-CT dataset. It contains 48260 and 15589 CT slices from 282 normal and 95 COVID-19 patients respectively. They reported binary classification accuracy 98.49% for slice level, and 95.5% (234 out of 245) for patient level. The study did not consider other viral pneumonia cases. The binary classification between normal class and infected class is simpler than the multiclass classification between normal class, COVID-19 infected class and other CAP class.

In 2021, Shahin Heidarian et al. [22] reported a two-stage capsule network named COVID-FACT for COVID-19 detection at the patient level. It used the COV-CT-MD dataset [23] of CT images of multiple classes. In the first stage, it classifies between infected and non-infected slices, and in the second stage, it classifies patient between COVID and non-COVID categories. The network consists of four convolutional layers and three capsule layers in both stages. The image features are extracted using convolution layers and fed into capsule layers. Each capsule in capsule layers forward the object existence probability and passes from one layer to next higher layers. A patient-level classification is done based on average voting with varying threshold degrees. They reported 91.83% accuracy at the patient-level classification at stage 2. Therefore, there is need of computation model that gives better accuracy than the state-of-the-art methods reported in the literature.

For such multiclass classification the challenge is- it is more challenging to differentiate between COVID-19 and CAP infection slices even for radiologist because COVID-19 infected slices and CAP infected slices both have infected regions with similar image features [19]. We aim to employ CNN network to do this task to differentiate between COVID-19 and CAP infection slices that may help radiologist for better diagnosis.

Motivation: A very few methods discussed in literature considered Covid-19 and CAP cases together. Even these studies considered small number of images from each class. The reported accuracy is up to 91.83% in patient level. There is a scope to improve the accuracy further. Our objective is to develop a multiclass classifier that is capable to identify Normal, Covid-19 and CAP cases considering large number of images.

Contribution of this study are- a) we developed an optimized multi-class CNN model, Cov-CT-Net to classify Normal, COVID-19, and other Community-Acquired Pneumonia from CT slices. Our optimized network requires as less as 1/69th number of trainable parameters compared to COVID-FACT network reported by Heidarian et al. [22] in 2021. b) This deep learning-based model is tested extensively on the publicly available dataset COV-CT-MD. It can predict with more than 98% accuracy for slice level. The model gave us a patient-level accuracy of 83.47% in the COVID-19 class. The accuracy is better than the one reported by Heidarian et al. [22] on the same dataset using CNN. We also extend the slice label predictions to the patient level by majority voting on the average probability of detected infected CT slices of a patient. c) The CT dataset contains many unlabelled slices. It consists of COVID infected as well as non-infected slices. The model labels all these unlabelled slices (in the COVID-19 class of patient level) and verified by radiologist. These slices may be used as pseudo labelled slices in semi-supervised learning.

The article is organized as follows. Section 2, Materials and Method section explains the model, Cov-CT-Net. Section 3, Experimental results are shown, and section 4 concludes the article.

2. MATERIALS AND METHOD

This section describes the model design, dataset, and performance analysis.

2.1 DATASET

In this paper, we use the COV-CT-MD [23] dataset, which is publicly available. The dataset consists of slice-level, lobe-level and patient-level data and includes slice-level CT images of 169 COVID-19 patients, 76 Normal, and 60 CAP cases in DICOM (Digital Imaging and Communications in Medicine) format. Each image size is 512x512, and the bit depth is 8. It has slice and lobe labels for 54 COVID-19 and 25 CAP patients. In this study, we consider slice-level data only. Fig. 1 illustrates a CT slice image of normal, COVID-19 infected, and CAP-infected chest radiography.

(a) (b) (c)

Fig.1. The CT images of lung- a) CAP infected, b) COVID-19 infected, c) Normal

A few datasets are publicly available on CT images of COVID-19 subjects. Most of them contain images about Covid and Non-covid cases. Besides, the datasets contain only infected slices in Covid cases rather than the whole volume. The COV-CT-MD dataset in our study contains three class data and provides adequate labelling suitable to train the deep learning-based models. Moreover, Afsar et al. [13] reported this is the first dataset with slice, lobe, and patient-level labelling. We have used this dataset to carry out experiment.

2.2 DATA SELECTION

In the dataset, there are 3779 infected slices of 54 patients infected with COVID-19, 1178 infected slices of 25 patients infected with Community-Acquired Pneumonia, and 18392 non-infected slices of normal cases of 76 persons. The slice level and patient level data is presented in Table.1 and Table.2. For the present study, non-infected slices have been taken only from normal cases.

Table.1. Slice level data available in the COV-CT-MD dataset

	COVID-19 cases	**CAP cases**	**Normal cases**
Labelled data	3779	1178	18392
Unlabelled data	16891	5231	-

Table.2. Patient level data in the COV-CT-MD dataset

	Labelled data		**Unlabelled data**	
	Patient ID	**Total**	**Patient ID**	**total**
COVID-19 cases	P001 to P054	54	P055 to P169	115
CAP cases	CAP001 to CAP025	25	CAP026 to CAP060	35
Normal cases	NORMAL001 to NORMAL076	76	-	-

The involvement of each positional CT slices on 54 COVID-19 cases, considering the slices took from positional index 1 to 200, depicted in Fig.2 as slice histogram. It is observed from the slice histogram that infected slices range from index 11 to 118. Also, it is observed that slices ranging from 68 to 88 are mostly infected.

The average number of CT slices per patient is 149, and the average number of COVID-19 infected slices per patient is 70, with a minimum of 9 (≈7%) and a maximum of 137 (≈86%). Using this observation, we considered a patient as normal or not infected if less than 5% of slices of the patient are infected for patient-level prediction.

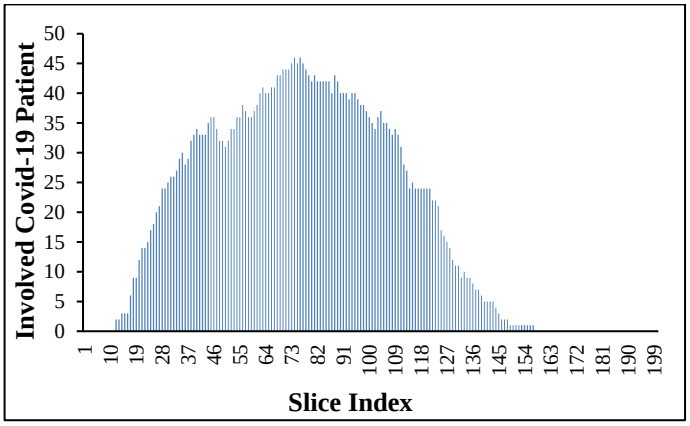

Fig.2. CT Slice Histogram of involved COVID-19 Cases

The infected slices are randomly selected from COVID-19 and CAP cases to train the model. The number of CT slices in CAP cases is 1178. But we need at least 3500 slices (the required number of slices 2500 for training, 500 for validation and 500 for testing) so we used data augmentation to generate more samples from these 1178 samples of the CAP class for data balancing. The CAP slices are augmented with rotation (-30, +30), shearing (-20, +20) and scaling (0.8, 1.2). A total of 3534 images are generated using the augmentation techniques. From these augmented slices only 1322 slices are randomly chosen along with original 1178 slices (total 2500) for training of the model. We considered 3705 slices of normal cases, 3779 slices of COVID-19 infected cases, and 4712 slices of CAP cases for the study. For the training dataset total 7500 slices are considered- 2500 slices from each class of normal, COVID-19 and CAP cases. For validation and test dataset, 500 number of samples from each class total 1500 samples are considered. The details is given in Table.3.

Table.3. Slice level data used in experimentation

	COVID-19	**CAP**	**Normal**	**Total**
Training dataset	2500	2500	2500	7500
Validation dataset	500	500	500	1500
Test dataset	500	500	500	1500

For slice-level labeling of unlabeled data in the dataset using the model, we ignored the slices where the lung is invisible, or visibility is very narrow. As the number of CT slices of each patient differs, we ignored 10% slices from the start and end index for prediction of class label and labelled those ignored slices as non-infected.

2.3 PREPROCESSING

Each DICOM image is resized into 256x256 to fit the model and saved in a NumPy array for fast training. As CNN is robust against noise or missing data, we used this resized image into the model without further pre-processing.

2.4 MODEL DESIGN

This study uses a five-layer Convolutional Neural Network to predict Normal Covid and other Community-Acquired

Pneumonia (CAP) cases on CT slices. The model architecture is shown in Fig.3.

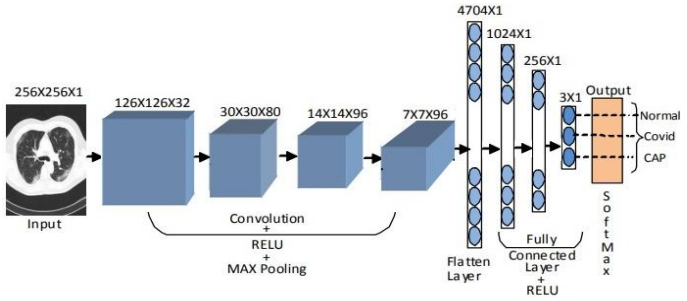

Fig.3. Cov-CT-Net architecture

2.5 OPTIMIZER

We use an Adaptive Moment Estimation (Adam) [24] optimizer in this study. It works by estimating the first and second moments of the gradient to adapt the learning rate for each weight of the neural network using Eq.(1) and Eq.(2).

$$m_t = \beta_1 m_{t-1} + (1-\beta_1) g_t \tag{1}$$

$$v_t = \beta_2 v_{t-1} + (1-\beta_2) g_t^2 \tag{2}$$

where β_1 and β_2 are the decay rate of the average of the gradient of first and second moments respectively and g is the gradient on the current mini batch. Finally, weights, W are updated at t^{th} epoch using Eq.(3).

$$w_t = w_{t-1} - \eta \frac{\hat{m}_t}{\sqrt{\hat{v}_t} + \varepsilon} \tag{3}$$

where $\hat{m}_t$ and $\hat{v}_t$ are bias corrected first and second moments. Bias correction is done by Eq.(4) and Eq.(5).

$$\hat{m}_t = \frac{m_t}{1-\beta_1^t} \tag{4}$$

$$\hat{v}_t = \frac{v_t}{1-\beta_2^t}, \tag{5}$$

where, η is the step size and ε is a very small number. We have set $\beta_1 = 0.9$, $\beta_2 = 0.999$ and $\varepsilon = 1e^{-8}$. The Adam optimizer has faster computation and low memory requirements than other optimizers. It is suitable for high volume image dataset [14].

2.6 LOSS FUNCTION

The loss function used to train the Cov-CT-Net model is sparse categorical cross-entropy based on mean squared error. Sparse categorical cross-entropy has the same loss function as categorical cross-entropy. The only difference is in representing output labels. The loss for M number of classes is computed by Eq.(6).

$$L = -\sum_{j=1}^{M} y_j \log(\hat{y}_j) \tag{6}$$

where y is the actual target and y hat is the predicted target. Considering N training samples, the cost function is given by Eq.(7).

$$L = -\frac{1}{N} \sum_{i}^{N} \sum_{j=1}^{M} y_{ij} \log(\hat{y}_{ij}) \tag{7}$$

2.7 MODEL ARCHITECTURE

In this study, an eight-layer Convolutional Neural Network (CNN) named Cov-CT-Net is designed to detect COVID-19 using CT images. There are four types of layers present in the CNN-Convolution layer, Pooling layer, Flatten layer, and Fully Connected layer (FCN) [15]. The model extracts features hierarchically. At first, low-level features are extracted, then mid-level and high-level features are extracted.

Convolution layer is the main building block of CNN to extract input features. Features are extracted using several filters, known as kernels. Kernel performs convolution operation, which is the summation of the element by the element dot product between inputs and the kernels. Four convolution layers are used in the Cov-CT-Net model, followed by ReLU activation after each convolution operation to introduce non-linearity. Rectified Linear Unit (ReLU) is an activation function in the model. A rectified linear equation is given by Eq.(8).

$$f(u) = \max(0, u) \tag{8}$$

Pooling layers perform dimensionality reduction of feature maps generated from convolution layers using kernels. MaxPooling selects the maximum value within the receptive field between the kernel and inputs.

Flatten layer transforms the feature maps to single dimensional array of size 4704. The one-dimensional vector is used as input in fully connected layers for classification.

Table.4. Hyper-parameters of Convolution and Pooling layers and Input-Output volume

	Convolution				Max Pooling		Volume	
Layer	No. of Filter	Kernel size	Padding	Stride	Kernel size	Stride	Input Volume	Output Volume
1	32	3	0	1	3	2	256x256x1	126x126x32
2	80	5	0	2	3	2	126x126x32	30x30x80
3	96	3	1	2	2	1	30x30x80	14x14x96
4	96	3	1	1	2	2	14x14x96	7x7x96

The three Fully Connected layers (FCN) in order are used in dimensions 1024, 256 and 3 to classify inputs into COVID-19, CAP, and Normal classes. A softmax [15] activation function is used in the last layer to get predictions with probability 0 to 1 in each class by the Eq.(9).

$$S(y)_i = \frac{\exp(y_i)}{\sum_{j=1}^{M} \exp(y_j)} \quad (9)$$

The Cov-CT-Net CNN model architecture is illustrated in Fig.3. The different hyper-parameters and feature dimensions are presented in Table.4. The number of filters affects the depth of output. The stride is the distance or the number of pixel that the kernel moves over the input matrix.

3. EXPERIMENTAL RESULTS

A dataset of 10500 samples (3500 random samples from each class) is used for experimentation. For model training, testing, and validation 7500, 1500 and 1500 number of slices are used. Class-wise distribution of slices is shown in Table 3. The performance of the model is evaluated in terms of accuracy with different batch size. The Fig.4 shows that the model gives the best result with batch size of 8.

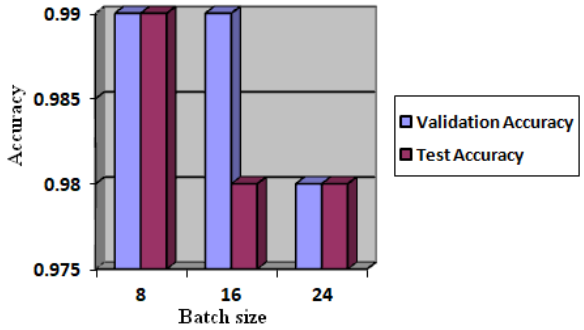

Fig.4. Validation accuracy and test accuracy with different batch size

The model is trained with batch size of eight. The accuracy and loss graph are shown in Fig.5 and Fig.6, respectively. In Fig.5 it can be observed that the model converges after 12 to 13 epochs with high training and validation accuracy.

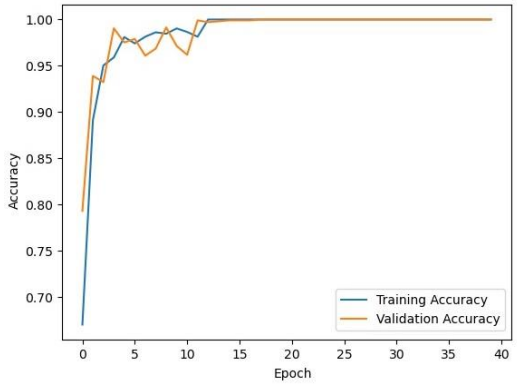

Fig.5. Accuracy vs no. of epoch graph of Cov-CT-Net

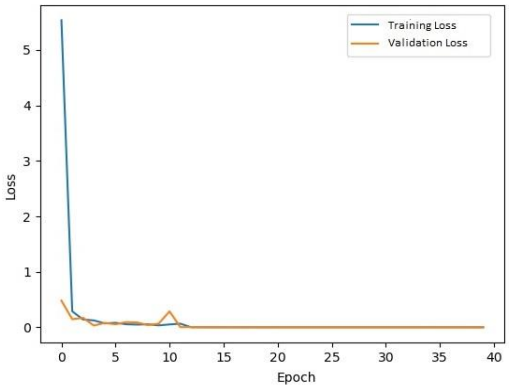

Fig.6. Loss vs no of epoch graph of Cov-CT-Net

The Receiver Operating Characteristic (ROC) [27] curve is widely used in medicine field to find the presence or absence of patient disease based on test result. The curve is constructed by connecting the coordinate points using "false positive rate (FP)" as x-axis and "true positive rate (TP)" in y-axis. FP refers the proportion of CT slices that are not infected but are incorrectly classified as infected. TP refers those proportions of CT-slices that are infected and correctly classified. The 45 degree diagonal line corresponds to random classification. The Area Under the Curve (AUC) gives the accuracy measurement of test result. On 45 degree diagonal AUC=0.5 Therefore, AUC must be greater than 0.5. The ROC curve of the Cov-CT-Net model presented in Fig.7 where (a) represents the classification performance of the model considering Normal class vs Rest (Covid-19 and CAP cases), (b) represents Covid-19 class vs Rest (Normal and CAP cases) and (c) represents CAP class vs Rest (Normal and Covid-19).

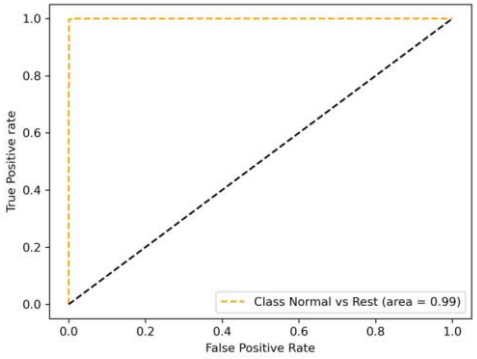

(a)

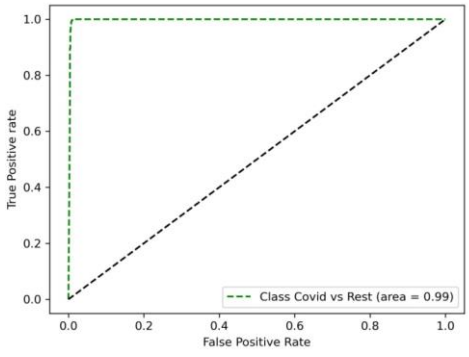

(b)

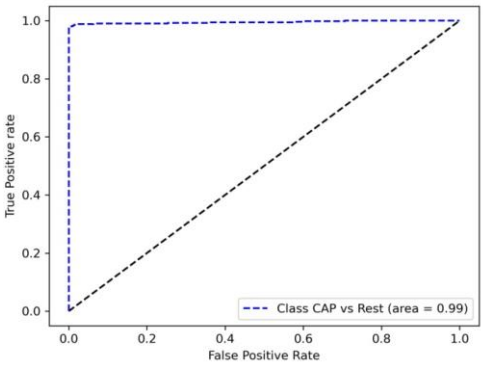

(c)

Fig.7. Receiver Operating Characteristic Curve (a) Normal Class vs Rest (b) COVID-19 vs Rest (c) CAP vs Rest

From the ROC curves the model has the ability to distinguish between different classes with 0.99 probability which is supported by the AUC.

To assess the performance of Cov-CT-Net, 1500 CT slices, 500 from each class, are used, which are not included in the training set. The test classification result and confusion matrix [25] are given in Table 5 and 6, respectively. The Cov-CT-Net model obtains a test accuracy of 0.99.

Table.5. Classification performance of Cov-CT-Net

	Precision	**Recall**	**F1 score**
Class 0 (Normal)	1	1	1
Class 1 (COVID-19 Infected)	1	0.98	0.99
Class 2 (CAP Cases)	0.97	1	0.99

Table.6. Confusion matrix of Cov-CT-Net

	Class0	**Class1**	**Class2**
Class0(Normal)	499	0	2
Class1(COVID-19 Infected)	1	500	11
Class2(CAP Infected)	0	0	487

From Table.6, we can see that the model is able to identify Covid-19 infected slices with 100% precision. The small 3x3 filters can capture the highly localized lesions of GGO like imaging features which are present mostly in lower lobes as hazy transparent opacities. The 5x5 filter with two stride in the second convolution layer designed to capture scattered lesions and consolidation pattern present in Covid-19 infected lungs.

The Table.6 shows that one slice belonging to the normal class is misclassified to COVID-19 infected class. At the same time, all COVID-19 infected slices are properly classified. The classification result of CAP-infected slices shows 11 slices are miss-classified as COVID-19. This miss-classification is not a surprise as the pattern in CAP CT slices is similar to COVID-19 infection. The GGO and Airspace Consolidation are present in CAP and COVID-19 [20].

We extend the model prediction from the slice level to the patient level. The patient-level predictions are carried out by averaging the probabilities of slice-level class predictions of infected CT slices for a patient. We con-sider the patient-level prediction normal whenever infected slices are less than 4% of the total CT slices examined and considered these predicted infections as model errors. Fig.8 demonstrates the precisions achieved experimentally on different cutoff values in Covid-19 Class. Based on our experiment and as reported by Nan Yu et al. [26], we choose 4% cutoff. For other cases, we account for majority voting between the COVID-19 and CAP classes.

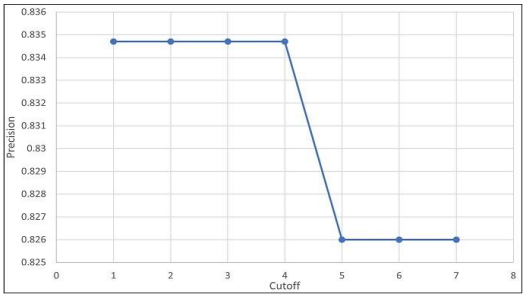

Fig.8. Precision Vs Cutoff in COVID-19 Class

We labelled the unlabelled slices at the patient level based on averaging the predicted class probabilities. Table 7 shows the result of patient-level prediction.

Table.7. Performance of patient level prediction of Cov-CT-Net

Patient Index	**COVID-19**	**CAP**
Patient Index	P055 to P169	CAP026 to CAP060
Correct Prediction	96/115	14/35

The number of patient-level misclassification of COVID-19 case as CAP case and Normal case is 18 (15.65%) and 1 (0.8%) respectively.

The clinical data of the patient id P091, misclassified as Normal class, recorded as Myalgia, Diarrhoea, and RTPCR not done. Among the misclassified CAP cases, the clinical record is shown in Table.8.

Table.8. Clinical record of misclassified samples

Patient ID	**Clinical record**	**RTPCR status**
P056	Cough	Not done
P061	Fatigue, Cough, History of myasthenia gravis	Positive
P062	Flu-like symptoms	Not done
P075	Cough, Known case of scleroderma	Not done
P079	Cough, Fever, History of Flu-like symptoms	Not done
P081	Dyspnoea	Not done
P099	Dyspnoea, Cough, History of colon cancer	Not done
P104	Cough	Not done
P107	Headache, Myalgia, Nausea	Not done
P111	Cough	Positive
P131	Cough	Not done
P132	Cough	Not done
P136	Fever	Not done

P148	Dyspnoea	Not done
P151	Abdominal pain	Positive
P155	Fever, Chills	Not done
P169	Dyspnoea	Not done

Two RTPCR-positive cases are misclassified as CAP cases. Most of the other misclassified patients have cough as one of the symptoms.

The performance of our model is compared with the state-of-the-art models reported in the literature. We have tested the CNN model on COVID-CT-MD dataset to classify Normal, COVID-19 and other Community Acquired Pneumonia (CAP) cases in slice level and patient level. The Cov-CT-Net model achieved 99% accuracy in slice level and 83.3% accuracy in patient level on test set. A comparative study with CNN-based COVID-FACT proposed by Shahin Heidarian et al. [22] on same dataset is given in Table.9. Our model gives better accuracy than the CNN-based COVID-FACT model [22]. Also, the Cov-CT-Net model requires 5,297,747 number of trainable parameters whereas the CNN-based COVID-FACT model [22] requires 365,806,660 number of trainable parameters (which is almost 69 times of Cov-CT-Net). Therefore, the Cov-CT-Net is much simple one and it requires less computation time for training.

Table.9. Comparison between Covid-Fact [22] and our Cov-CT-Net model

Method	**Slice level accuracy**	**Patient level precision (COVID-19 cases)**	**Patient level precision (CAP cases)**	**Trainable parameters**
CNN-based Covid-Fact	79.74%	82.40% (14/17)	25% (2/8)	365,806,660
Cov-CT-Net	99.00%	83.48% (96/115)	40% (14/35)	5,297,747

A detailed comparison is given with other state of the art models for COVID-19 detection using CT or CR images with our model. It is shown in Table 10.

Mahmud et al. [20] reported a multiclass classification model for slice level. They have considered 305 images from each class. The size of the dataset is small compared to the size of the dataset used in the experiment. They reported 90.20% accuracy in slice level classification, but they did not report patient level accuracy. The slice level accuracy of our model is better than other state of the art model.

Rahimzadeh et al. [21] reported the method as binary class classification. They did not consider Community-Acquired Pneumonia cases. The binary classification between normal class and infected class is simpler than the multiclass classification between normal class, COVID-19 infected class and CAP class. As COVID-19 infected slices and CAP infected slices have infection regions with similar image properties so it is challenging task to differentiate between COVID-19 and CAP infected slices. Again, the patient level accuracy reported by Rahimzadeh et al. [21] is between Normal case and COVID-19 infected case. In patient level multiclass scenario our method performs better.

Table.10. Comparison study between our Cov-CT-Net model and other state-of-art models

Title	**Dataset type**	**Size of dataset**	**Accuracy (Slice level)**	**Accuracy (Patient level)**
Mahmud et al. [20] in 2020	Multi-class (Normal, Non-COVID viral pneumonia, non-COVID bacterial pneumonia and COVID-19 class)	305 CR images from each class	90.20%	Not reported
Rahimzadeh et al. [21] in 2021	Binary class (Normal and COVID-19)	48160 CT from normal and 15589 from COVID-19	98.49%	95.5% (234/245)*
Cov-CT-Net	Multi-class (Normal, COVID-19, CAP)	18447 CT slices from normal and 4962 from infected	99.00%	83.47% (96/115)

*Accuracy reported by Rahimzadeh et al. [21] is for binary classification between Normal case and COVID-19 infected case

4. CONCLUSION

This study designed an efficient yet simple multi-class CNN model, Cov-CT-Net to classify between COVID-19 cases, other Community-Acquired Pneumonia (CAP) infection and Normal cases at patient level using chest CT slices. The model is trained and tested on the publicly available dataset COVID-CT-MD. It achieves accuracy of 99% on test data at the slice level. The patient-level labelling is decided using average voting of all detected infected CT slices of a patient. The proposed model gave a patient-level accuracy of 83.47% in the COVID-19 class. Our optimized Cov-CT-Net network requires 5,297,747 number of trainable parameters. Whereas recently reported COVID-FACT network applied on the same dataset requires 365,806,660 number of trainable parameters which is almost 69 times that of the Cov-CT-Net. The patient level accuracy is better than the state-of-the-art method reported using the same dataset. The model labels the unlabelled slices of the dataset. These labelled slices may be used as a pseudo labelled slices in semi-supervised learning.

REFERENCES

[1] World Health Organization (WHO), "WHO Coronavirus (COVID-19) Dashboard", Available at https://www.covid19.who.int, Accessed on 2023.

[2] X. Xu and G. Lang, "A Deep Learning System to Screen Novel Coronavirus Disease 2019 Pneumonia", *Engineering*, Vol. 6, No. 10, pp. 1122-1129, 2020.

[3] M.V.M.K Atalla and I.A. Moonesar, "Detection of COVID-19 using Deep Learning Techniques and Cost Effectiveness Evaluation: A survey", *Frontiers in Artificial Intelligence*, Vol. 5, pp. 1-13, 2022.

[4] Y. Fang P. Pang and W. Ji, "Sensitivity of Chest CT for COVID-19: Comparison to RT-PCR", *Radiology*, Vol. 296, No. 2, pp. 115-117, 2020.

[5] H.Y. Wong, K.W. Chiu, T.W. Chung and E.Y. Lee, "Frequency and Distribution of Chest Radiographic Findings in Patients Positive for COVID-19", *Radiology*, Vol. 296, No. 2, pp. 72-78, 2020.

[6] A. Borakati, A. Perera and T. Sood, "Diagnostic Accuracy of X-ray Versus CT in COVID-19: A Propensity-Matched Database Study", *BMJ Open*, Vol. 10, No. 11, pp. 42946-42953, 2020.

[7] M. Chung and A. Jacobi, "CT Imaging Features of 2019 Novel Corona Virus (2019-nCoV)", *Radiology*, Vol. 295, No. 1, pp. 202-207, 2020.

[8] N. Yu, S. Cai and Y. Guo, "Lung Involvement in Patients with Corona Virus Disease-19 (COVID-19): A Retrospective Study based on Quantitative CT Findings", *Chinese Journal of Academic Radiology*, Vol. 3, pp. 102-107, 2020.

[9] S. Inui and Y. Uwabe, "Chest CT Findings in Cases from the Cruise ship Diamond Princess with Coronavirus Disease (COVID-19)", *Radiology: Cardiothoracic Imaging*, Vol. 2, No. 2, pp. 200110-200123, 2020.

[10] M.Y. Ng and C.K. Hui, "Imaging Profile of the COVID-19 Infection: Radiologic Findings and Literature Review", *Radiology: Cardiothoracic Imaging*, Vol. 2, No. 1, pp. 34-43, 2020.

[11] H. Shi, Y. Fan and C. Zheng, "Radiological Findings from 81 patients with COVID-19 Pneumonia in Wuhan, China: a Descriptive Study", *The Lancet Infectious Diseases*, Vol. 20, No. 4, pp. 425-434, 2020.

[12] C. Janiesch, P. Zschech and K. Heinrich, "Machine Learning and Deep Learning", *Electronic Markets*, Vol. 31, No. 3, pp. 685-695, 2021.

[13] G. Carneiro and L. Yang, "Review of Deep Learning Methods in Mammography, Cardiovascular, and Microscopy Image Analysis", *Proceedings of International Conference on Deep Learning and Convolutional Neural Networks for Medical Image Computing*, pp. 11-32, 2017.

[14] G. Litjens and C.I. Sanchez, "A Survey on Deep Learning in Medical Image Analysis", *Medical Image Analysis*, Vol. 42, pp. 60-88, 2017.

[15] R. Yamashita and K. Togashi, "Convolutional Neural Networks: An Overview and Application in Radiology", *Insights into Imaging*, Vol. 9, pp. 611-629, 2018.

[16] M.V. Herk, "Errors and Margins in Radiotherapy", in *Proceeding of Seminar in Radiation Oncology*, WB Saunders, Vol. 14, No. 1, pp. 52-64, 2004.

[17] S. Yang, L. Jiang, Z. Cao and F. Shan, "Deep Learning for Detecting Corona Virus Disease 2019 (COVID-19) on High-Resolution Computed Tomography: A Pilot Study", *Annals of Translational Medicine*, Vol. 8, No. 7, pp. 1-12, 2020.

[18] L. Wang and A. Wong, "Covid-Net: A Tailored Deep Convolutional Neural Network Design for Detection of Covid-19 Cases from Chest X-Ray Images", *Scientific Reports*, Vol. 10, No. 1, pp. 1-12, 2020.

[19] S. Hu and H. Ye, "Weakly Supervised Deep Learning for Covid-19 Infection Detection and Classification from CT Images", *IEEE Access*, Vol. 8, pp. 118869-118883, 2020.

[20] T. Mahmud and S.A. Fattah, "CovXNet: A Multi-Dilation Convolutional Neural Network for Automatic COVID-19 and other Pneumonia Detection from Chest X-Ray Images with Transferable Multi-Receptive Feature Optimization", *Computers in Biology and Medicine*, Vol. 122, pp. 103869-103877, 2020.

[21] M. Rahimzadeh and S.M. Sakhaei, "A Fully Automated Deep Learning-Based Network for Detecting COVID-19 from a New and Large Lung CT Scan Dataset", *Biomedical Signal Processing and Control*, Vol. 68, pp. 102588-102595, 2021.

[22] S. Heidarian, S.F. Atashzar, A. Oikonomou and A. Mohammadi, "COVID-FACT: A Fully-Automated Capsule Network-Based Framework for Identification of COVID-19 Cases from Chest CT Scans", *Frontiers in Artificial Intelligence*, Vol. 4, pp. 598932-598943, 2021.

[23] P. Afshar and A. Mohammadi, "COVID-CT-MD, COVID-19 Computed Tomography Scan Dataset Applicable in Machine Learning and Deep Learning", *Scientific Data*, Vol. 8, No. 1, pp. 121, 2021.

[24] A. Khadidos and G. Tsaramirsis, "Analysis of Covid-19 Infections on a CT Image using Deepsense Model", *Frontiers in Public Health*, Vol. 8, pp. 599550-599562, 2020.

[25] M. Grandini, E. Bagli and G. Visani, "Metrics for Multi-Class Classification: An Overview", *Proceedings of International Conference on Deep Learning*, pp. 5756-5764, 2020.

[26] N. Yu and Y. Guo, "Lung Involvement in Patients with Coronavirus Disease-19 (COVID-19): A Retrospective Study based on Quantitative CT Findings", *Chinese Journal of Academic Radiology*, Vol. 3, pp. 102-107, 2020.

[27] F.S. Nahm, "Receiver Operating Characteristic Curve: Overview and Practical use for Clinicians", *Korean journal of Anesthesiology*, Vol. 75, No. 1, pp. 25-36, 2022.